High resolution 3D Tau-p transform by matching pursuit

Weiping Cao and Warren S. Ross, Shearwater GeoServices*

Summary

The 3D Tau-p transform is of vital significance for processing seismic data acquired with modern wide azimuth recording systems. This paper presents a 3D high resolution Tau-p transform based on the matching pursuit algorithm. 3D seismic data are first transformed to the frequency domain, and a sparse set of f-p_x-p_y coefficients are iteratively inverted by matching pursuit. When the data are spatially aliased, the inversion results are weighted by a total energy mask. The numerical examples demonstrate this scheme achieves a high resolution Tau-p transform that represents the input data accurately and handles spatial aliasing properly.

Introduction

The Tau-p transform, also called the linear Radon transform, has been a very important tool in seismic data processing. Its applications range from linear noise removal to de-ghosting and data interpolation/regularization. The Tau-p transform is usually formulated as an inverse problem to solve for the Tau-p coefficients that best represent the input data under certain criteria,

$$d = Lm \ . \tag{1}$$

In the above equation, m is the tau-p model and L is the transform operator. Unlike the Fourier transform, the basis for the Tau-p transform is not orthogonal. Therefore traditional L2 norm based inversion algorithms provide a low resolution transformation, especially when the data sampling and aperture are not ideal. Various authors developed 2D high resolution Radon transform schemes (Thorson and Claerbout 1985; Sacchi and Ulrych 1995; Cary, 1998; Trad et al., 2003, Wang et al., 2009) by imposing sparsity constraints in the time or frequency domain, and the above issue has been effectively mitigated for 2D seismic data.

Though 2D Tau-p transform has been widely used in seismic processing, its 2D plane wave assumption cannot handle the 3D curvature variations with azimuth present in 3D seismic data. Therefore the Tau-p transform needs to be extended to 3D to process 3D seismic data, especially those data acquired with wide azimuth recording systems. Zhang and Lu (2013) developed an accelerated high resolution 3D Tau-p transform with an efficient spatial transform scheme followed by iterative thresholding of the inverted Tau-p coefficients. Wang and Nimsaila (2014) proposed a fast progressive sparse Tau-p transform: a low-rank optimization is applied for inversion stability and efficiency, and aliasing is handled by progressively driving the inversion for high frequencies with the low frequency results.

This paper proposes a matching pursuit method for 3D Tau-p transform. The matching pursuit algorithm provides an approximate L0 norm solution to inverse problems, and has been very successful with FK domain seismic interpolation/regularization (Xu et al., 2005;Ozbek et al., 2010; Nguyen and Winnett, 2011; Hollander et al., 2012; Schonewille et al., 2013). We choose a matching pursuit approach because of its proven performance in the FK context, and because it has a straightforward implementation. Also, to properly handle spatial aliasing, the total energy of each p trace is computed and used as a mask for the matching pursuit solution.

Method

The matching pursuit algorithm builds up a sparse solution to the inverse problem by iteratively picking the strongest component in the model residue. For the Tau-p transform implementation, matching pursuit is implemented on frequency slices after the input data are transformed into the frequency domain.

In the frequency domain, the terms in equation 1 are formulated as: input data $d = d(f, x_i, y_i)$, where (x_i, y_i) represent the spatial coordinates of trace number i; $m = m(f, p_x^j, p_y^j)$ is the Tau-p coefficient for the jth p pair. The transform operator L is expressed as

$$L_{i,j} = e^{-i \cdot 2\pi \cdot f \, (p_x^j \cdot x_i + p_y^j \cdot y_i)} \ . \tag{2}$$

The adjoint transform is formulated as

$$\tilde{m}(f, p_x^j, p_y^j) = L^H d = \sum_i e^{i \cdot 2\pi \cdot f \, (p_x^j \cdot x_i + p_y^j \cdot y_i)} d(f, x_i, y_i) \ , \tag{3}$$

The algorithm is implemented as follows:

1. Initialize the data residual with the input data
2. Calculate the adjoint model by applying the adjoint of operator L to the residual
3. Select the strongest component in the adjoint model and add it to the estimated solution
4. Inverse transform the selected component into the data (space) domain, and update the data residual by subtracting this transformed component
5. Go to step 2 if residual level is not low enough. Otherwise exit iteration.

To avoid a large number of temporal Fourier transform operations, the input seismic data are transformed into the frequency space domain, and matching pursuit iterations are implemented for each frequency slice.

In 3D seismic acquisition, the seismic data are usually aliased in the crossline direction, and spatial aliasing brings a serious challenge to the Tau-p transform. To overcome this issue, for each p_x, p_y trace we compute the total energy during the matching pursuit iterations, creating a mask over the entire p_x, p_y space. Then in later iterations, this mask is used as a model-space weight for the inversion. This process is repeated periodically throughout the inversion iterations until a satisfactory residual is achieved.

Figures 1- 3 show a simple synthetic example to compare Tau-p transform results obtained with the matching pursuit algorithm and a Cauchy-like sparse inversion scheme with some similarities to that of Sacchi and Ulrych (1995). As illustrated in Figure 2, the matching pursuit algorithm delivers a Tau-p transform with higher resolution and more accurate amplitude. Also these two Tau-p panels are transformed back to seismic traces to check the fidelity of the forward transform by checking the round-trip errors. Figure 3 shows the round-trip errors scaled by 10 displayed at the same range as Figure 1. The worst error amplitude of the Cauchy-like approach is over ten times that for the matching pursuit scheme. This test demonstrates that relative to the Cauchy-like approach shown here the matching pursuit algorithm provides a Tau-p transform that has higher resolution *and* represents the data more accurately.

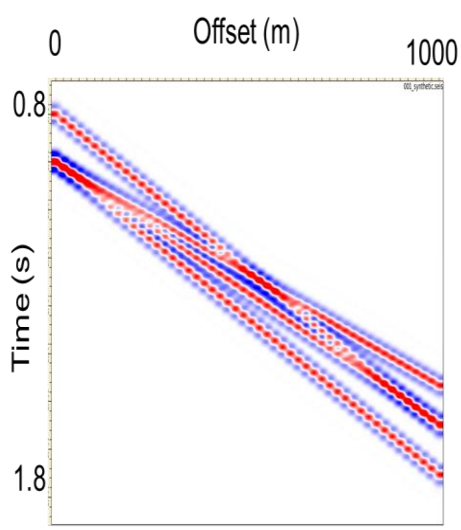

Figure 1: synthetic data with 4 linear events

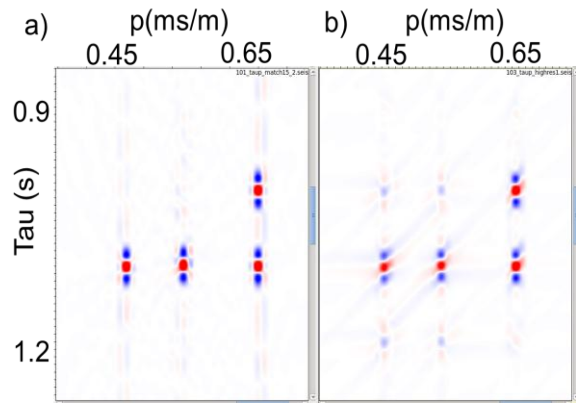

Figure 2: Tau-p panels for a) matching pursuit method and b) Cauchy-like method

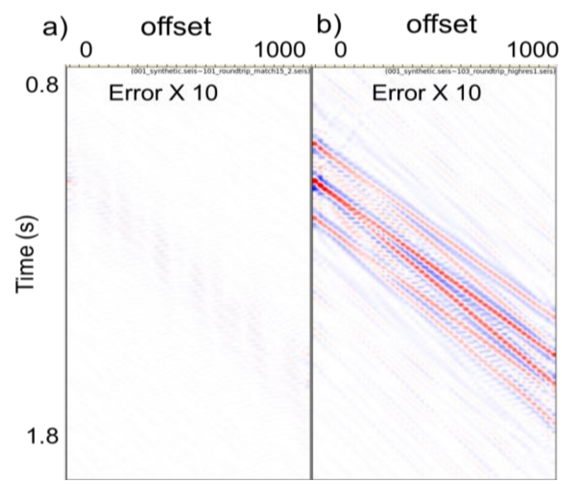

Figure 3: Tau-p transform round-trip error for a) match pursuit method and b) Cauchy-like method

Figures 4-6 show a 3D synthetic example to illustrate the performance of this anti-aliasing scheme. The trace spacing in the inline and crossline direction is 10 m, and the wavelet is a Ricker wavelet with maximum frequency 50 Hz. The dense crossline sampling in Figure 4 is decimated to 30 m to generate an aliased input for the Tau-p transform, and the Tau-p coefficients are used to interpolate the data back to the dense geometry. Figure 5 shows that without the anti-aliasing scheme, a significant amount of error is introduced at the interpolated trace locations. By contrast, the error at the input trace locations is very low, which indicates a good data match in Tau-p transform. When the anti-aliasing step is applied, the interpolation error is greatly reduced, as Figure 6 shows.

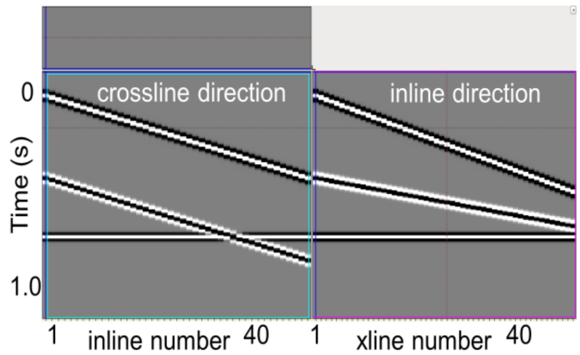

Figure 4: inline and crossline views of the synthetic data prior to crossline downsampling from 10 m to 30 m.

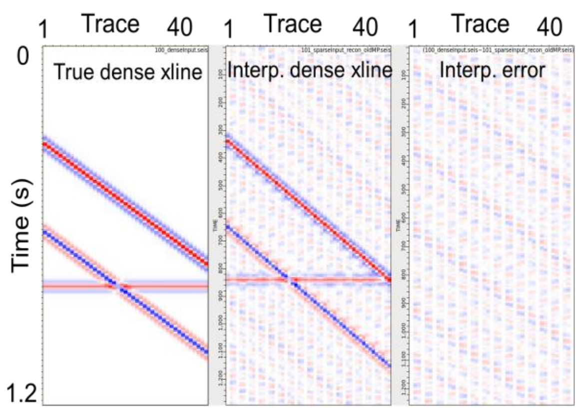

Figure 5: interpolation error for Tau-p without anti-aliasing

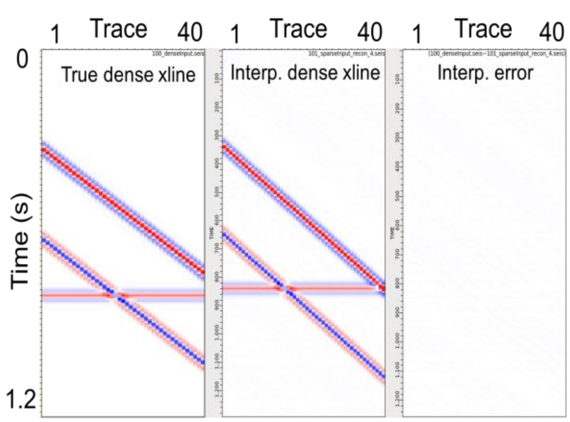

Figure 6: interpolation error for Tau-p with anti-aliasing

Field data example

We applied this sparse Tau-p transform algorithm to a deep-water 3D marine shot gather to test its performance on interpolation. Acquisition consisted of ten cables with a spacing of 150 m, and 12.5 m channel spacing along the cable. For the test, the data is first decimated by a factor of two in the cable direction to generate a sparse dataset. As the three-slice view in Figure 7 shows the dataset is badly sampled in both the inline and crossline direction. The FK spectrum in Figure 8 shows the data is clearly aliased in the inline direction.

The high resolution 3D Tau-p transform is applied to the decimated data, and the resultant Tau-p coefficients are used to interpolate back to the original dense sampling in the cable direction, and compared with the true dense data. Figures 9 and 10 demonstrate the interpolation results for a near and a far cable. Note that although this is a 3D transform, the interpolation was performed only in one (the inline) direction, not the very sparse crossline direction.

We also test the interpolation performance for different percentages of the Tau-p coefficient threshold. As shown in Figure 11 for the center part of the data (trace 25-80) the RMS interpolation error drops to 10-15% if we use 0.5% of the Tau-p coefficients, and increasing the threshold percentage to 1% brings little improvement to the error level. There is no significant difference for the near and far cables. The valleys of the "V" shapes are locations where input traces are available and we have data control to reach the best interpolation fit. The interpolation error on the near traces is at or below 10%. This is a 2 to 1 interpolation, and the crossline direction is very badly aliased (with 150 cable spacing). Overall we think the interpolation performance is reasonable considering the input data is seriously aliased in both directions.

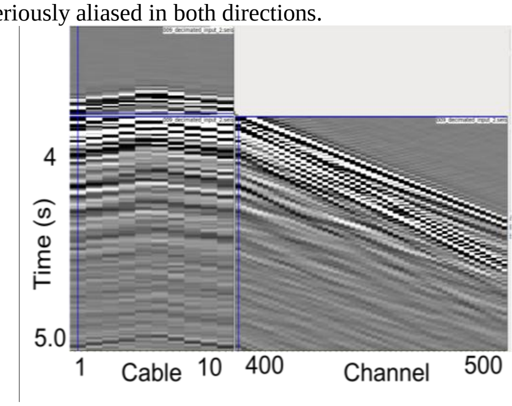

Figure 7: 3D sparse input data for interpolation The average cable spacing is 150, and after decimation the group interval is 25 m.

High resolution 3D Tau-p transform

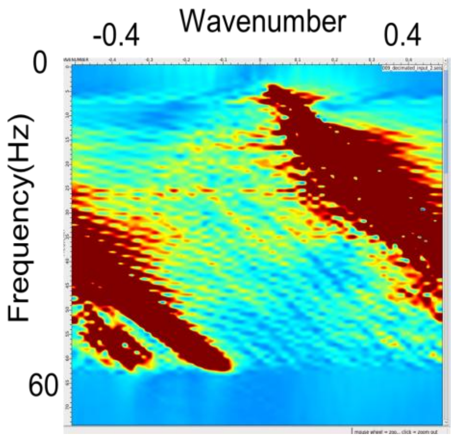

Figure 8: FK spectrum of the decimated input in the inline direction

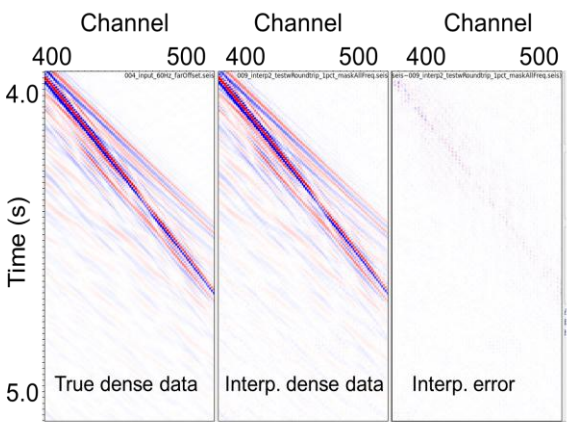

Figure 9: Interpolation for a far cable: true dense cable (left), interpolated dense cable (center) and the interpolation error (right).

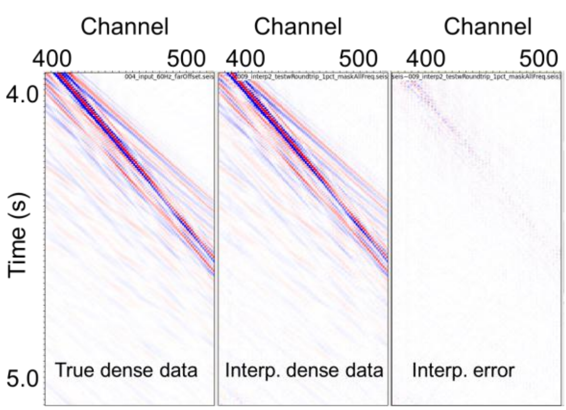

Figure 10: Interpolation for a near cable: true dense cable (left), interpolated dense cable (center) and the interpolation error (right).

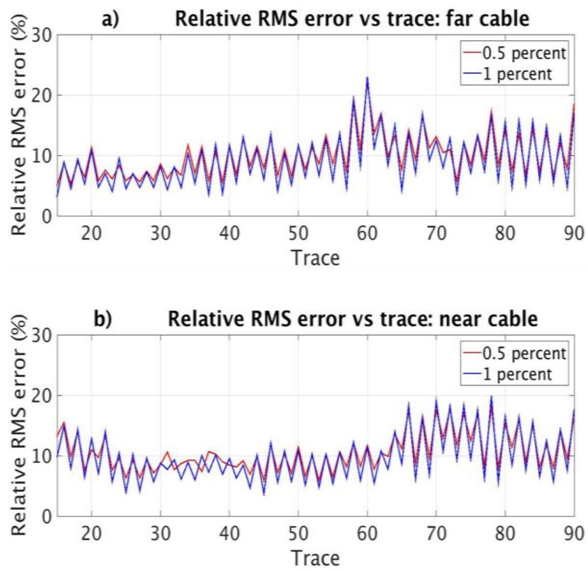

Figure 11: interpolation error vs traces for two different threshold percentages (0.5% and 1%) of Tau-p coefficients for interpolation

Conclusions

A high resolution 3D Tau-p transform scheme is developed to process sparse 3D seismic data. With the matching pursuit algorithm and an anti-aliasing strategy based on total energy in the Tau-p plane, a high resolution Tau-p representation of the aliased 3D data can be achieved. Numerical examples demonstrate improved resolution in the Tau-p transform and a more accurate data representation. The application of this scheme to field data interpolation/regularization shows promising results.

Acknowledgments

The authors would like to Sergio Grion for many helpful discussions and Shearwater Geoservices for the permission of publish this work.

References

Cary, P., 1998, The simplest discrete Radon transform: 68th Annual International Meeting, SEG Expanded Abstracts, 1999–2002

Nguyen, T., and R. Winnett, 2011, Seismic interpolation by optimally matched Fourier components: 81st Annual International Meeting, SEG, Expanded Abstracts, 3085–3089

Özbek, A., M. Vassallo , A. K. Özdemir, D. Molteni, and Y. K. Alp, 2010, Anti-alias optimal interpolation with priors: 80th Annual International Meeting, SEG, Expanded Abstracts, 3401–3405.

Sacchi, M., and T. Ulrych, 1995, High-resolution velocity gathers and offset space reconstruction: Geophysics, 60, 1169–1177

Schonewille, M., Zhimei Yan, Martin Bayly and Richard Bisley, 2013, Matching pursuit Fourier interpolation using priors derived from a second data set: 83rd Annual International Meeting, SEG Expanded Abstracts, 3651-3654

Trad, D., T. Ulrych, and M. Sacchi, 2003, Latest views of the sparse Radon transform: Geophysics, 68,386–399

Thorson, R., and Claerbout, J., 1985, Velocity-stack and slant-stack stochastic inversion: Geophysics, 50, 2727–2741

Wang, J., M. Ng, and M. Perz, 2010, Seismic data interpolation by greedy local Radon transform: Geophysics,75, no. 6, WB225–WB234

Wang, P. and K. Nimsaila, 2014, Fast progressive sparse Tau-P transform for regularization of spatially aliased seismic data: 84th Annual International Meeting, SEG Expanded Abstracts, 3589-3592

Xu, S., Y. Zhang, D. L. Pham, and G. Lambaré, 2005, Antileakage Fourier transform for seismic data regularization: Geophysics,70, no. 4, V87–V95

Zhang, Y., and W. Lu, 2014, 2D and 3D prestack seismic data regularization using an accelerated sparse time-invariant Radon transform: Geophysics,79, no. 5, V165–V177